PHYSICAL REVIEW D **85,** 034034 (2012)

Baryonium study in heavy baryon chiral perturbation theory

Yue-De Chen[1,*] and Cong-Feng Qiao[1,2,†]

[1]*Department of Physics, Graduate University, Chinese Academy of Sciences, YuQuan Road 19A, 100049, Beijing, China*
[2]*Theoretical Physics Center for Science Facilities, CAS, YuQuan Road 19B, 100049, Beijing, China*

(Received 20 February 2011; published 22 February 2012)

To see whether a heavy baryon and an antibaryon can form a bound state, the heavy baryonium, we study the two-pion exchange interaction potential between them within the heavy baryon chiral perturbation theory. The obtained potential is applied to calculate the heavy baryonium masses by solving the Schrödinger equation. We find it is true that the heavy baryonium may exist in a reasonable choice of input parameters. The uncertainties remaining in the potential and their influences on the heavy baryonium mass spectrum are discussed.

DOI: 10.1103/PhysRevD.85.034034 PACS numbers: 12.39.Fe, 13.75.Gx, 14.20.Pt

I. INTRODUCTION

The quark model has achieved great success in describing the experimentally observed hadronic structures to a large extent. And the quark potential in between a quark and an antiquark deduced from QCD can explain the meson spectrum quite well. Many of the states predicted by the potential model were discovered in experiment, and the theoretical predictions are in good agreement with experimental data, especially in the charmonium and bottomonium sectors [1–3], where the masses of the charm and bottom quarks are heavy enough to be treated nonrelativistically. However, things became confused after the discovery of $X(3872)$ in 2003 by Belle [4], which was later confirmed by *BABAR* [5]. In recent years, a series of unusual states in the charmonium sector, such as $Y(4260)$, $Y(4360)$, $Y(4660)$, and $Z^{\pm}(4430)$, were observed in experiment [6]. Because of their extraordinary decay nature, it is hard to embed them into the conventional charmonium spectrum, which leads people to treat them as exotic rather than quark-quark bound states. The typical scenarios in explaining these newly found states include treating $Y(4260)$ as a hybrid charmonium [7], as a $\chi_c\rho^0$ molecular state [8], as a conventional $\Psi(4S)$ [9], as an $\omega\chi_{c1}$ molecular state [10], as a $\Lambda_c\bar{\Lambda}_c$ baryonium state [11], as a D_1D or D_0D^* hadronic molecule [12], and as a P-wave tetraquark $[cs][\bar{c}\,\bar{s}]$ state [13]; $Y(4360)$ is interpreted as a candidate for the charmonium hybrid or an excited D-wave charmonium state, the 3^3D_1 [14], and an excited state of baryonium [15]; $Y(4660)$ is suggested to be the excited S-wave charmonium states, the 5^3S_1 [14] and 6^3S_1 [16], a baryonium state [15,17], a $f_0(980)\Psi'$ bound state [18,19], a 5^3S_1–4^3D_1 mixing state [20], and also a tetraquark state [21,22]. There has recently been much research on an ''exotic'' heavy quarkonium study in experiment and theory. To know more about recent progress in this respect and to have a more complete list of references, one can see e.g. recent reviews [23,24] and references therein.

In the baryonium picture, the triquark clusters are baryonlike, but not necessarily colorless. In the pioneering works of heavy baryonium for the interpretation of newly observed exotic structures [11,15], there have been only phenomenological and kinematic analyses, but without dynamics. In this work we attempt to study the heavy baryonium interaction potential arising from two-pion exchanges in the framework of heavy baryon chiral perturbation theory (HBCPT) [25]. The paper is organized as follows. In Sec. II we present the formalism for the heavy baryon-baryon interaction study; in Sec. III we perform the numerical study for the mass spectrum of the possible baryonium with the potential obtained in the preceding section; Sec. IV is devoted to a summary and conclusions. For the sake of the reader's convenience, some of the formulas used are given in the Appendix.

II. FORMALISM

To obtain the heavy baryonium mass spectrum, we first start by extracting the baryon-baryon interaction potential using the same procedure as for the quark-quark interaction [1].

A. Heavy baryonium

In the heavy baryonium picture [15], Λ_c and Σ_c^0 are taken as basis vectors in two-dimensional space. The baryonia are loosely bound states of a heavy baryon and an antibaryon, namely,

$$\text{Triplet}: \begin{cases} B_1^+ \equiv |\Lambda_c^+\bar{\Sigma}_c^0\rangle \\ B_1^0 \equiv \frac{1}{\sqrt{2}}(|\Lambda_c^+\bar{\Lambda}_c^+\rangle - |\Sigma_c^0\bar{\Sigma}_c^0\rangle) \\ B_1^- \equiv |\bar{\Lambda}_c^+\Sigma_c^0\rangle \end{cases} \tag{1}$$

and

$$\text{Singlet}: B_0^0 \equiv \frac{1}{\sqrt{2}}(|\Lambda_c^+\bar{\Lambda}_c^+\rangle + |\Sigma_c^0\bar{\Sigma}_c^0\rangle). \tag{2}$$

*chenyuede-b07@mails.gucas.ac.cn
†qiaocf@gucas.ac.cn

Here, the transformation in this two-dimensional "C-spin" space is approximately invariant, which is in analogy to the invariance of isospin transformation in a proton and neutron system.

B. Effective chiral Lagrangian

The heavy baryon contains both light and heavy quarks, of which the light component exhibits the chiral property and the heavy component exhibits heavy symmetry. Therefore, it is plausible to tackle the problem of heavy baryon interaction through the heavy chiral perturbation theory. In the following we briefly review the gist of the HBCPT for later use.

In usual chiral perturbation theory, the nonlinear chiral symmetry is realized by making use of the unitary matrix

$$\Sigma = e^{(2iM/f_\pi)}, \tag{3}$$

where M is a 3×3 matrix composed of eight Goldstone-boson fields, i.e.,

$$M = \begin{pmatrix} \frac{1}{\sqrt{2}}\pi^0 + \frac{1}{\sqrt{6}}\eta & \pi^+ & K^+ \\ \pi^- & -\frac{1}{\sqrt{2}}\pi^0 + \frac{1}{\sqrt{6}}\eta & K^0 \\ K^- & \bar{K}^0 & -\frac{2}{\sqrt{6}}\eta \end{pmatrix}. \tag{4}$$

Here, f_π is the *pion* decay constant.

After the chiral symmetry is spontaneously broken, the Goldstone-boson interaction with the hadron is introduced through a new matrix [26,27]:

$$\xi = \Sigma^{1/2} = e^{(iM/f_\pi)}. \tag{5}$$

From ξ one can construct a vector field V_μ and an axial vector field A_μ with simple chiral transformation properties, i.e.,

$$V_\mu = \tfrac{1}{2}(\xi^\dagger \partial_\mu \xi + \xi \partial_\mu \xi^\dagger), \tag{6}$$

$$A_\mu = \frac{i}{2}(\xi^\dagger \partial_\mu \xi - \xi \partial_\mu \xi^\dagger). \tag{7}$$

For our aim, we work only on the leading order vector and axial vector fields in the expansion of ξ in terms of f_π; they are

$$V_\mu = \frac{1}{f_\pi^2} M \partial_\mu M, \tag{8}$$

$$A_\mu = -\frac{1}{f_\pi} \partial_\mu M. \tag{9}$$

For the heavy baryon, each of the two light quarks is in a triplet of flavor SU(3), and hence the baryons can be grouped into two different SU(3) multiplets, the sixtet and the antitriplet. The symmetric sixtet and the antisymmetric triplet can be constructed using 3×3 matrices [27]; they are

$$B_6 = \begin{pmatrix} \Sigma_c^{++} & \frac{1}{\sqrt{2}}\Sigma_c^+ & \frac{1}{\sqrt{2}}\Xi_c^{\prime +} \\ \frac{1}{\sqrt{2}}\Sigma_c^+ & \Sigma_c^0 & \frac{1}{\sqrt{2}}\Xi_c^{\prime 0} \\ \frac{1}{\sqrt{2}}\Xi_c^{\prime +} & \frac{1}{\sqrt{2}}\Xi_c^{\prime 0} & \Omega_c^0 \end{pmatrix} \tag{10}$$

and

$$B_{\bar{3}} = \begin{pmatrix} 0 & \Lambda_c & \Xi_c^+ \\ -\Lambda_c & 0 & \Xi_c^- \\ -\Xi_c^+ & -\Xi_c^- & 0 \end{pmatrix}, \tag{11}$$

respectively.

Introducing six coupling constants g_i, $i = 1, 6$, the general chiral-invariant Lagrangian then reads [25]

$$\begin{aligned} \mathcal{L}_{\mathcal{G}} = {} & \tfrac{1}{2}\mathrm{tr}[\bar{B}_{\bar{3}}(i\not{v} - M_{\bar{3}})B_{\bar{3}}] + \mathrm{tr}[\bar{B}_6(i\not{v} - M_6)B_6] \\ & + \mathrm{tr}[\bar{B}_6^{*\mu}[-g_{\mu\nu}(i\not{v} - M_6^*) + i(\gamma_\mu D_\nu + \gamma_\nu D_\mu) \\ & - \gamma_\mu(i\not{v} + M_6^*)\gamma_\nu]B_6^{*\nu}] + g_1\mathrm{tr}(\bar{B}_6\gamma_\mu\gamma_5 A^\mu B_6) \\ & + g_2\mathrm{tr}(\bar{B}_6\gamma_\mu\gamma_5 A^\mu B_{\bar{3}}) + \mathrm{H.c.} + g_3\mathrm{tr}(\bar{B}_{6\mu}^* A^\mu B_6) \\ & + \mathrm{H.c.} + g_4\mathrm{tr}(\bar{B}_{6\mu}^* A^\mu B_{\bar{3}}) + \mathrm{H.c.} \\ & + g_5\mathrm{tr}(\bar{B}_6^{\nu *}\gamma_\mu\gamma_5 A^\mu B_{6\nu}^*) + g_6\mathrm{tr}(\bar{B}_{\bar{3}}\gamma_\mu\gamma_5 A^\mu B_{\bar{3}}). \end{aligned} \tag{12}$$

Here, $B_{6\nu}^*$ is a Rarita-Schwinger vector-spinor field for a spin-$\frac{3}{2}$ particle; $M_{\bar{3}}$, M_6, M_6^* represent heavy baryon mass matrices of the corresponding fields. With the help of the vector current V_μ defined in Eq. (8), we may construct the covariant derivative D_μ, which acts on the baryon field as

$$D_\mu B_6 = \partial_\mu B_6 + V_\mu B_6 + B_6 V_\mu^T, \tag{13}$$

$$D_\mu B_{\bar{3}} = \partial_\mu B_{\bar{3}} + V_\mu B_{\bar{3}} + B_{\bar{3}} V_\mu^T, \tag{14}$$

where V_μ^T stands for the transpose of V_μ. Thus, the couplings of the vector current to heavy baryons that are relevant to our task take the following form:

$$\begin{aligned} \mathcal{L}_{\mathcal{E}_1} &= \frac{1}{2}\mathrm{tr}(\bar{B}_{\bar{3}} i\gamma^\mu V_\mu B_{\bar{3}}) \\ &= \frac{1}{2f_\pi^2}\bar{\Lambda}_c i\gamma^\mu(\pi^0\partial_\mu\pi^0 + \pi^-\partial_\mu\pi^+ + \pi^+\partial_\mu\pi^-)\Lambda_c \end{aligned} \tag{15}$$

and

$$\begin{aligned} \mathcal{L}_{\mathcal{E}_2} &= \frac{1}{2}\mathrm{tr}(\bar{B}_{\bar{3}} B_{\bar{3}} i\gamma^\mu V_\mu^T) \\ &= \frac{1}{2f_\pi^2}\bar{\Lambda}_c\Lambda_c i\gamma^\mu(\pi^0\partial_\mu\pi^0 + \pi^-\partial_\mu\pi^+ + \pi^+\partial_\mu\pi^-). \end{aligned} \tag{16}$$

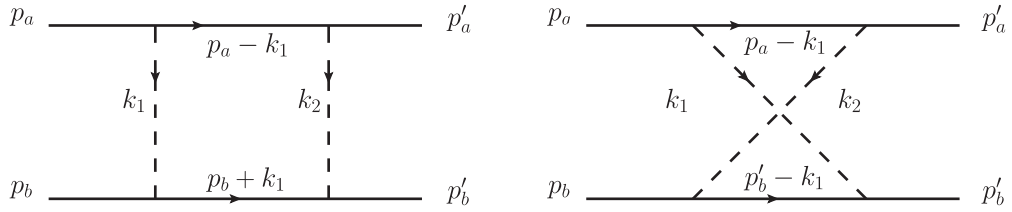

FIG. 1. Schematic diagrams which contribute to the baryonium potential.

According to the heavy quark symmetry, there are four constraint relations among the six coupling constants of the Lagrangian of Eq. (12), i.e.,

$$g_6 = 0, \qquad g_3 = \frac{\sqrt{3}}{2} g_1, \qquad g_5 = -\frac{3}{2} g_1, \qquad g_4 = -\sqrt{3} g_2, \tag{17}$$

which means the number of independent couplings is then reduced to two. In this work, we employ g_1 and g_2 for the numerical evaluation, as was done in Ref. [25].

Here, to get the dominant interaction potential we restrict our effort only to the pion exchange processes, as usual. Notice that the couplings of the pion to spin-$\frac{3}{2}$ and spin-$\frac{1}{2}$ baryons and of the pion to two spin-$\frac{1}{2}$ baryons take a similar form; in the following we merely present the spin-$\frac{3}{2}$ and spin-pion baryon-pion couplings for illustration, i.e.,

$$\mathcal{L}_1 = \frac{g_3}{\sqrt{2} f_\pi} \bar{\Sigma}_c^{0*\mu} \partial_\mu \pi^0 \Sigma_c^0 + \text{H.c.}, \tag{18}$$

$$\mathcal{L}_2 = -\frac{g_3}{\sqrt{2} f_\pi} \bar{\Sigma}_c^{+*\mu} \partial_\mu \pi^+ \Sigma_c^0 + \text{H.c.}, \tag{19}$$

$$\mathcal{L}_3 = \frac{g_4}{f_\pi} \bar{\Sigma}_c^{++*\mu} \partial_\mu \pi^+ \Lambda_c^+ + \text{H.c.}, \tag{20}$$

$$\mathcal{L}_4 = -\frac{g_4}{f_\pi} \bar{\Sigma}_c^{0*\mu} \partial_\mu \pi^- \Lambda_c^+ + \text{H.c.}, \tag{21}$$

$$\mathcal{L}_5 = -\frac{g_4}{f_\pi} \bar{\Sigma}_c^{+*\mu} \partial_\mu \pi^0 \Lambda_c^+ + \text{H.c.} \tag{22}$$

To get the pion and two spin-$\frac{1}{2}$ baryon couplings, one only needs to replace the $\Sigma_c^{*\mu}$ by Σ_c, g_3 by g_1, g_4 by g_2, and insert $\gamma^\mu \gamma_5$ in between the two baryon fields in Eqs. (18)–(22).

C. Baryonium potential from two-pion exchange

To obtain the heavy baryon-baryon interaction potential in configuration space, we start by writing down the two-body scattering amplitude in the center-of-mass frame (CMS), i.e. by taking $\mathbf{p}_a = -\mathbf{p}_b$ and $\mathbf{p}'_a = -\mathbf{p}'_b$. In the CMS the total and relative four-momenta are defined as

$$P = (p_a + p_b) = (p'_a + p'_b) = (E, 0), \tag{23}$$

$$p = \tfrac{1}{2}(p_a - p_b) = (0, \mathbf{p}), \tag{24}$$

$$p' = \tfrac{1}{2}(p'_a - p'_b) = (0, \mathbf{p}'). \tag{25}$$

To perform the calculation, it is convenient to introduce some new variables as functions of $\mathbf{p}$ and $\mathbf{p}'$, i.e.,

$$\mathcal{W}(\mathbf{p}) = E_a(\mathbf{p}) + E_b(\mathbf{p}), \tag{26}$$

$$\mathcal{W}(\mathbf{p}') = E_a(\mathbf{p}') + E_b(\mathbf{p}'), \tag{27}$$

$$F_E(\mathbf{p}, p_0) = \tfrac{1}{2}E + p_0 - E(\mathbf{p}) + i\delta, \tag{28}$$

where δ is an infinitesimal quantity introduced in the so-called $i\delta$ prescription. Following the same procedure as in Refs. [28,29], it is straightforward to write down the baryon-baryon scattering kernels, shown as box and crossed diagrams in Fig. 1,

$$K_{\text{box}} = -\frac{1}{(2\pi)^2}(E - \mathcal{W}(\mathbf{p}'))(E - \mathcal{W}(\mathbf{p})) \int dp'_0 dp_0 dk_{20} dk_{10} d^3\mathbf{k}_2 d^3\mathbf{k}_1 \frac{i}{(2\pi)^4} \delta^4(p - p' - k_1 - k_2) \frac{1}{k_2^2 - m^2 + i\delta} \times \frac{1}{F_E(\mathbf{p}', p'_0) F_E(-\mathbf{p}', -p'_0)} \frac{\Gamma_j \Gamma_i \Gamma_i \Gamma_j}{F_E(\mathbf{p} - \mathbf{k}, p_0 - k_{10}) F_E(-\mathbf{p} + \mathbf{k}, -p_0 + k_{10})} \frac{1}{F_E(\mathbf{p}, p_0) F_E(\mathbf{p}, -p_0))} \frac{1}{k_1^2 - m^2 + i\delta}, \tag{29}$$

$$K_{\rm cross} = -\frac{1}{(2\pi)^2}(E - \mathcal{W}(\mathbf{p}'))(E - \mathcal{W}(\mathbf{p}))\int dp_0' dp_0 dk_{20} dk_{10} d^3\mathbf{k}_2 d^3\mathbf{k}_1 \frac{i}{(2\pi)^4}\delta^4(p - p' - k_1 - k_2)$$
$$\times \frac{1}{k_2^2 - m^2 + i\delta}\frac{1}{F_E(\mathbf{p}', p_0')F_E(-\mathbf{p}', -p_0')}\frac{\Gamma_j\Gamma_i\Gamma_j\Gamma_i}{F_E(\mathbf{p} - \mathbf{k}, p_0 - k_{10})F_E(-\mathbf{p}' - \mathbf{k}, -p_0' - k_{10})}$$
$$\times \frac{1}{F_E(\mathbf{p}, p_0)F_E(-\mathbf{p}, -p_0)}\frac{1}{k_1^2 - m^2 + i\delta}. \quad (30)$$

Here, m corresponds to the pion mass and $\Gamma_{i,j}$ are heavy baryon-pion interaction vertices that can be read off from the Lagrangian in Eqs. (18)–(22). In the case of spin-$\frac{3}{2}$ intermediate states,

$$\Gamma_j\Gamma_i\Gamma_i\Gamma_j = \left(\frac{g_4}{f_\pi}\right)^4 \bar{u}(-p)k_2^\mu u_\mu(p - k_1)\bar{u}_\nu(p - k_1)$$
$$\times k_1^\nu u(p)\bar{v}(p)(-k_1^\alpha)v_\alpha(-p + k_1)\bar{v}_\beta(-p + k_1)$$
$$\times k_2^\beta v(-p), \quad (31)$$

and in the case of spin-$\frac{1}{2}$ intermediates,

$$\Gamma_j\Gamma_i\Gamma_i\Gamma_j = \left(\frac{g_2}{f_\pi}\right)^4 \bar{u}(-p)\gamma_\mu\gamma_5 k_2^\mu u(p - k_1)\bar{u}(p - k_1)$$
$$\times \gamma_\nu\gamma_5 k_1^\nu u(p)\bar{v}(p)\gamma_\alpha\gamma_5(-k_1^\alpha)v(-p + k_1)$$
$$\times \bar{v}(-p + k_1)\gamma_\beta\gamma_5 k_2^\beta v(-p). \quad (32)$$

Integrating over p_0', p_0, k_{10}, and k_{20} in Eq. (29), one obtains the interaction kernel of the box diagram at order $\mathcal{O}(\frac{1}{M_H})$,

$$K_{\rm box} = -\frac{1}{(2\pi)^3}\int \frac{d^3\mathbf{k}_1 d^3\mathbf{k}_2}{4E_{\mathbf{k}_1}E_{\mathbf{k}_2}}\frac{\Gamma_j\Gamma_i}{E_{\mathbf{p}-\mathbf{k}_1} + E_{\mathbf{p}} - W + E_{\mathbf{k}_1}}$$
$$\times \frac{\Gamma_i\Gamma_j}{E_{\mathbf{p}}' + E_{\mathbf{p}-\mathbf{k}_1} - W + E_{\mathbf{k}_2}}$$
$$\times \frac{1}{E_{\mathbf{p}} + E_{\mathbf{p}'} - W + E_{\mathbf{k}_1} + E_{\mathbf{k}_2}}, \quad (33)$$

where M_H represents one of the heavy baryon masses, $M_{\Lambda_c^+}$, $M_{\Sigma_c^0}$, or $M_{\Sigma_c^*}$; $E_{\mathbf{p}-\mathbf{k}_1} = \sqrt{(\mathbf{p} - \mathbf{k}_1)^2 + M_{\Sigma_c^*}^2}$ is the intermediate state energy; $E_{\mathbf{k}_1} = \sqrt{\mathbf{k}_1^2 + m^2}$ and $E_{\mathbf{k}_2} = \sqrt{\mathbf{k}_2^2 + m^2}$ are two pions' energies; and $W = 2E(\mathbf{p})$. With the same procedure, we can get the interaction kernel of the crossed diagram, i.e.,

$$K_{\rm cross} = -\frac{1}{(2\pi)^3}\int \frac{d^3\mathbf{k}_1 d^3\mathbf{k}_2}{4E_{\mathbf{k}_1}E_{\mathbf{k}_2}}\frac{\Gamma_j\Gamma_i}{E_{\mathbf{p}-\mathbf{k}_1} + E_{\mathbf{p}} - W + E_{\mathbf{k}_1}}$$
$$\times \frac{\Gamma_j\Gamma_i}{E_{\mathbf{p}}' + E_{\mathbf{p}'+\mathbf{k}_1} - W + E_{\mathbf{k}_1}}$$
$$\times \frac{1}{E_{\mathbf{p}} + E_{\mathbf{p}'} - W + E_{\mathbf{k}_1} + E_{\mathbf{k}_2}}. \quad (34)$$

Next, since what we are interested in are the heavy baryons, we can further implement the nonrelativistic reduction on spinors with the help of vertices given in Eqs. (18)–(22). In the end, the nonrelativistic reduction for $\Lambda_c^+\Sigma_c^{+*}\pi^0$ and $\Lambda_c^+\Sigma_c^+\pi^0$ couplings gives

$$i\left(\frac{g_4}{f_\pi}\right)\bar{u}(p_2)u_\mu(p_1)(p_2 - p_1)^\mu = -i\left(\frac{g_4}{f_\pi}\right)\mathbf{S}^\dagger\cdot\mathbf{q} \quad (35)$$

and

$$i\left(\frac{g_2}{f_\pi}\right)\bar{u}(p_2)\gamma_\mu\gamma_5 u(p_1)(p_2 - p_1)^\mu = i\left(\frac{g_2}{f_\pi}\right)\boldsymbol{\sigma}_1\cdot\mathbf{q}, \quad (36)$$

respectively. Here, $\mathbf{q} = \mathbf{p}_2 - \mathbf{p}_1$ and $\mathbf{S}^\dagger$ is the spin-$\frac{1}{2}$ to spin-$\frac{3}{2}$ transition operator.

In the process of deriving the $\Lambda_c^+ - \bar{\Lambda}_c^+$ potential, the Σ_c^+ and Σ_c^{+*} are taken into account as intermediate states. Using Eqs. (35) and (36) and the explicit forms of spinors given in the Appendix, we can readily obtain the reduction forms for the Σ_c^+ intermediate state,

$$\bar{u}(-p)\gamma_\mu\gamma_5 k_2^\mu u(p - k_1)\bar{u}(p - k_1)\gamma_\nu\gamma_5 k_1^\nu u(p)\bar{v}(p)$$
$$\times \gamma_\alpha\gamma_5(-k_1^\alpha)v(-p + k_1)\bar{v}(-p + k_1)\gamma_\beta\gamma_5 k_2^\beta v(-p)$$
$$= (\mathbf{k}_1\cdot\mathbf{k}_2)^2 + (\boldsymbol{\sigma}_1\cdot\mathbf{k}_1\times\mathbf{k}_2)(\boldsymbol{\sigma}_2\cdot\mathbf{k}_1\times\mathbf{k}_2), \quad (37)$$

and the Σ_c^{+*} intermediate state in the box diagram,

$$\bar{u}(-p)k_2^\mu u_\mu(p - k_1)\bar{u}_\nu(p - k_1)k_1^\nu u(p)$$
$$\times \bar{v}(p)(-k_1^\alpha)v_\alpha(-p + k_1)\bar{v}_\beta(-p + k_1)k_2^\beta v(-p)$$
$$= \tfrac{4}{9}(\mathbf{k}_1\cdot\mathbf{k}_2)^2 - \tfrac{1}{9}(\boldsymbol{\sigma}_1\cdot\mathbf{k}_1\times\mathbf{k}_2)(\boldsymbol{\sigma}_2\cdot\mathbf{k}_1\times\mathbf{k}_2), \quad (38)$$

and in the crossed diagram

$$\bar{u}(-p)k_2^\mu u_\mu(p - k_1)\bar{u}_\nu(p - k_1)k_1^\nu u(p)$$
$$\times \bar{v}(p)(-k_1^\alpha)v_\alpha(-p + k_1)\bar{v}_\beta(-p + k_1)k_2^\beta v(-p)$$
$$= \tfrac{4}{9}(\mathbf{k}_1\cdot\mathbf{k}_2)^2 + \tfrac{1}{9}(\boldsymbol{\sigma}_1\cdot\mathbf{k}_1\times\mathbf{k}_2)(\boldsymbol{\sigma}_2\cdot\mathbf{k}_1\times\mathbf{k}_2), \quad (39)$$

respectively. Thus, the spinor reduction finally leads to an operator $\mathcal{O}_1(\mathbf{k}_1, \mathbf{k}_2)$, of which the variables $\mathbf{k}_1$ and $\mathbf{k}_2$ can be replaced by gradient operators $\boldsymbol{\nabla}_1$ and $\boldsymbol{\nabla}_2$ in

configuration space and acting on $\mathbf{r}_1$ and $\mathbf{r}_2$, respectively. This operator is expressed as

$$\begin{aligned}\mathcal{O}_1(\mathbf{k}_1,\mathbf{k}_2) &= c_1 O_1(\mathbf{k}_1,\mathbf{k}_2) + c_2 O_2(\mathbf{k}_1,\mathbf{k}_2)\\ &= c_1(\mathbf{k}_1\cdot\mathbf{k}_2)^2 + c_2(\boldsymbol{\sigma}_1\cdot\mathbf{k}_1\times\mathbf{k}_2)(\boldsymbol{\sigma}_2\cdot\mathbf{k}_1\times\mathbf{k}_2).\end{aligned} \tag{40}$$

Here, the decomposition coefficients c_1 and c_2 are given in Table I. The first part of Eq. (40) may generate the central potential, and the second part may generate the spin-spin coupling and the tensor potentials, which are explicitly shown in the Appendix.

To get the leading order central potential, e.g. for the Λ_c-$\bar{\Lambda}_c$ system, we first expand the energy in powers of $\frac{1}{M_H}$, but keep only the leading term, like

$$\begin{aligned}\frac{1}{E_{\mathbf{p}-\mathbf{k}_1}+E_{\mathbf{p}}-W+E_{\mathbf{k}_1}} &\approx \frac{1}{M_{\Sigma_c^*}+M_{\Lambda_c}-2M_{\Lambda_c}+E_{\mathbf{k}_1}}\\ &= \frac{1}{E_{\mathbf{k}_1}+\Delta_1},\end{aligned} \tag{41}$$

where $\Delta_1 = M_{\Sigma_c^*} - M_{\Lambda_c}$ represents the mass splitting. By virtue of the factorization in integrals given in the Appendix, we can then make a double Fourier transformation, i.e.,

$$V_C^B(r_1,r_2) = -\left(\frac{g_4^4}{f_\pi^4}\right)\iint\frac{d^3\mathbf{k}_1 d^3\mathbf{k}_2}{(2\pi)^6}\frac{\mathcal{O}_1(\mathbf{k}_1,\mathbf{k}_2)e^{i\mathbf{k}_1\mathbf{r}_1}e^{i\mathbf{k}_2\mathbf{r}_2}f(\mathbf{k}_1^2)f(\mathbf{k}_2^2)}{2E_{\mathbf{k}_1}E_{\mathbf{k}_2}(E_{\mathbf{k}_1}+\Delta_1)(E_{\mathbf{k}_2}+\Delta_1)(E_{\mathbf{k}_1}+E_{\mathbf{k}_2})}, \tag{42}$$

where the superscript B denotes the box diagram and the subscript C means the central potential. Similarly, one can get the central potential from the crossed diagram contribution,

$$V_C^C(r_1,r_2) = -\left(\frac{g_4^4}{f_\pi^4}\right)\iint\frac{d^3\mathbf{k}_1 d^3\mathbf{k}_2}{(2\pi)^6}\mathcal{O}_1(\mathbf{k}_1,\mathbf{k}_2)e^{i\mathbf{k}_1\mathbf{r}_1}e^{i\mathbf{k}_2\mathbf{r}_2}f(\mathbf{k}_1^2)f(\mathbf{k}_2^2)D, \tag{43}$$

where the superscript C denotes the crossed diagram and the subscript C means the central potential, and

$$\begin{aligned}D = \frac{1}{4E_{\mathbf{k}_1}E_{\mathbf{k}_2}}\Bigg[&\left(\frac{1}{(E_{\mathbf{k}_1}+\Delta_1)^2}+\frac{1}{(E_{\mathbf{k}_2}+\Delta_1)^2}\right)\frac{1}{E_{\mathbf{k}_1}+E_{\mathbf{k}_2}}\\ &+\left(\frac{1}{(E_{\mathbf{k}_1}+\Delta_1)^2}+\frac{1}{(E_{\mathbf{k}_2}+\Delta_1)^2}\right.\\ &\left.+\frac{2}{(E_{\mathbf{k}_1}+\Delta_1)(E_{\mathbf{k}_2}+\Delta_1)}\right)\frac{1}{E_{\mathbf{k}_1}+E_{\mathbf{k}_2}+2\Delta_1}\Bigg].\end{aligned} \tag{44}$$

In order to regulate the potentials, we have introduced form factors at each baryon-pion vertex. The resulting $f(\mathbf{k}^2)$ form factors appearing in Eqs. (42) and (43) will be given in Sec. III.

Taking a similar approach as given above, one can readily get the central potential in other interaction channels and also the tensor potential. Notice that, although there exists the one-pion exchange contribution in the Σ_c-Σ_c system, due to the $\gamma_\mu\gamma_5$ nature in the interaction vertex, it only contributes to the $\boldsymbol{\sigma}_1\cdot\boldsymbol{\sigma}_2$ term, which is not our concern in this work. Here we just focus on the central potential.

Besides box and crossed diagrams, there are also contributions from triangle and two-pion loop diagrams, as shown in Fig. 2. As in the box and crossed diagrams, after integrating over the energy component, we get the pion-pair contribution, shown in the left diagram of Fig. 2, as [30]

$$V_{\text{triangle}}(r_1,r_2) = \frac{g_4^2}{2f_\pi^4}\iint\frac{d^3\mathbf{k}_1 d^3\mathbf{k}_2}{(2\pi)^6}\frac{\mathcal{O}_2(\mathbf{k}_1,\mathbf{k}_2)(E_{\mathbf{k}_1}+E_{\mathbf{k}_2})e^{i\mathbf{k}_1\mathbf{r}_1}e^{i\mathbf{k}_2\mathbf{r}_2}f(\mathbf{k}_1^2)f(\mathbf{k}_2^2)}{E_{\mathbf{k}_1}E_{\mathbf{k}_2}(E_{\mathbf{k}_1}+\Delta_1)(E_{\mathbf{k}_2}+\Delta_1)}, \tag{45}$$

where the $\mathcal{O}_2(\mathbf{k}_1,\mathbf{k}_2) = (\mathbf{k}_1\cdot\mathbf{k}_2)$ from spinor reduction can be replaced in configuration space by the gradient operator $(\boldsymbol{\nabla}_1\cdot\boldsymbol{\nabla}_2)$. Similarly, the two-pion loop contribution, as shown in the right diagram of Fig. 2, reads

$$\begin{aligned}&V_{2\pi-\text{loop}}(r_1,r_2)\\ &\quad= \frac{1}{16f_\pi^4}\iint\frac{d^3\mathbf{k}_1 d^3\mathbf{k}_2}{(2\pi)^6}e^{i\mathbf{k}_1\mathbf{r}_1}e^{i\mathbf{k}_2\mathbf{r}_2}f(\mathbf{k}_1^2)f(\mathbf{k}_2^2)A.\end{aligned} \tag{46}$$

Here, $A = -\frac{1}{2E_{\mathbf{k}_1}} - \frac{1}{2E_{\mathbf{k}_2}} + \frac{2}{E_{\mathbf{k}_1}+E_{\mathbf{k}_2}}$. Expressing Eqs. (45) and (46) in the integral representation of $E_{\mathbf{k}_1}$, and making the Fourier transformation, one can then obtain the corresponding potentials.

III. NUMERICAL ANALYSIS

With the central potentials obtained in the preceding section, one can calculate the heavy baryonium spectrum by solving the Schrödinger equation. In our numerical evaluation, the MATLAB based package MATSLISE [31] is

TABLE I. The values of the coefficients c_1 and c_2 in the decomposition of operator $O(\mathbf{k}_1, \mathbf{k}_2)$ in Eq. (40). The upper table is for the spin-$\frac{1}{2}$ intermediate state case, and the lower table is for the spin-$\frac{3}{2}$ case.

Spin-1/2	c_1	c_2
Box	1	1
Cross	1	1

Spin-3/2	c_1	c_2
Box	4/9	−1/9
Cross	4/9	1/9

employed. The following inputs from the Particle Data Book [32] are used in the numerical calculation:

$$M_{\Lambda_c^+} = 2.286\ \text{GeV}, \quad M_{\Sigma_c^0} = 2.454\ \text{GeV}, \quad M_{\Sigma_c^*} = 2.518\ \text{GeV}, \quad f_\pi = 0.132\ \text{GeV}, \quad m = 0.135\ \text{GeV}, \tag{47}$$

and both spin-$\frac{1}{2}$ and spin-$\frac{3}{2}$ fermion intermediates are taken into account.

It is obvious that the main uncertainties in the evaluation of heavy baryonium remain in the couplings of Eq. (17). The magnitudes of the two independent couplings g_1 and g_2 were phenomenologically analyzed in Ref. [25], and two choices for them were suggested, i.e.,

$$g_1 = \tfrac{1}{3}, \qquad g_2 = -\sqrt{\tfrac{2}{3}} \tag{48}$$

and

$$g_1 = \tfrac{1}{3} \times 0.75, \qquad g_2 = -\sqrt{\tfrac{2}{3}} \times 0.75, \tag{49}$$

which implies that g_4 lies in the scope of 1 to 1.4, similar to what was estimated by Ref. [33] in the chiral limit.

A. Gaussian form factor case

The central potential from the two-pion exchange box diagram which can be regularized by the widely used Gaussian form factor $f(\mathbf{k}^2) = e^{-\mathbf{k}^2/\Lambda^2}$ reads

$$\begin{aligned} V_{CG}^B(r_1, r_2) &= -\left(\frac{g_4^4}{f_\pi^4}\right)\left[\frac{1}{\pi}\int_0^\infty \frac{d\lambda}{\Delta_1^2 + \lambda^2} O_1(\mathbf{k}_1, \mathbf{k}_2) F(\lambda, r_1) F(\lambda, r_2)\right. \\ &\quad \left. - \frac{2\Delta_1}{\pi^2} O_1(\mathbf{k}_1, \mathbf{k}_2) \int_0^\infty \frac{d\lambda}{\Delta_1^2 + \lambda^2} F(\lambda, r_1) \int_0^\infty \frac{d\lambda}{\Delta_1^2 + \lambda^2} F(\lambda, r_2)\right] \\ &= \sum_i V_{CGi}^B + \cdots. \end{aligned} \tag{50}$$

Details of the derivation of Eq. (50) from Eq. (42) can be found in the Appendix. There, the function $F(\lambda, r)$ is defined by Eq. (A11). And, similarly, the central potential from the two-pion exchange crossed diagram gives

$$V_{CG}^C(r_1, r_2) = -\left(\frac{g_4^4}{f_\pi^4}\right)\left[\frac{1}{\pi}\int_0^\infty \frac{d\lambda(\Delta_1^2 - \lambda^2)}{(\Delta_1^2 + \lambda^2)^2} O_1(\mathbf{k}_1, \mathbf{k}_2) F(\lambda, r_1) F(\lambda, r_2)\right] = \sum_i V_{CGi}^C + \cdots. \tag{51}$$

Here, the ellipsis represents the high singular terms in the $r_2 \to r_1 = r$ limit, which behave as higher order corrections to the potential and will not be taken into account in this work, but will be discussed elsewhere. The central potential of Eq. (50) is obtained in the case of the spin-$\frac{3}{2}$ intermediate state, and the explicit forms of V_{CGi} from the box diagram are

$$V_{CG1}^B = -\frac{g_4^4 \Lambda^7}{128\sqrt{2}\pi^{7/2} f_\pi^4 \Delta_1^2} e^{-(\Lambda^2 r^2/2)}, \tag{52}$$

$$V_{CG2}^B = -\frac{g_4^4 \Lambda^5}{16\sqrt{2}\pi^{7/2} f_\pi^4 \Delta_1^2 r^2} e^{-(\Lambda^2 r^2/2)}, \tag{53}$$

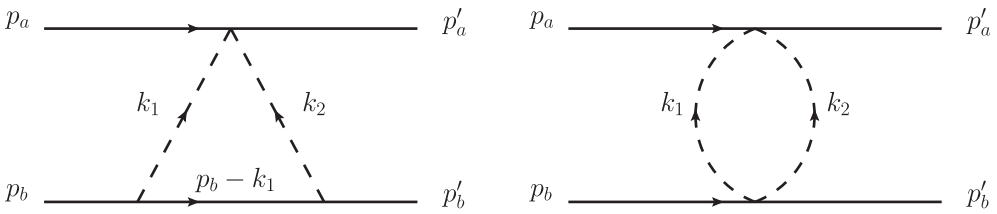

FIG. 2. The triangle and two-pion loop diagrams.

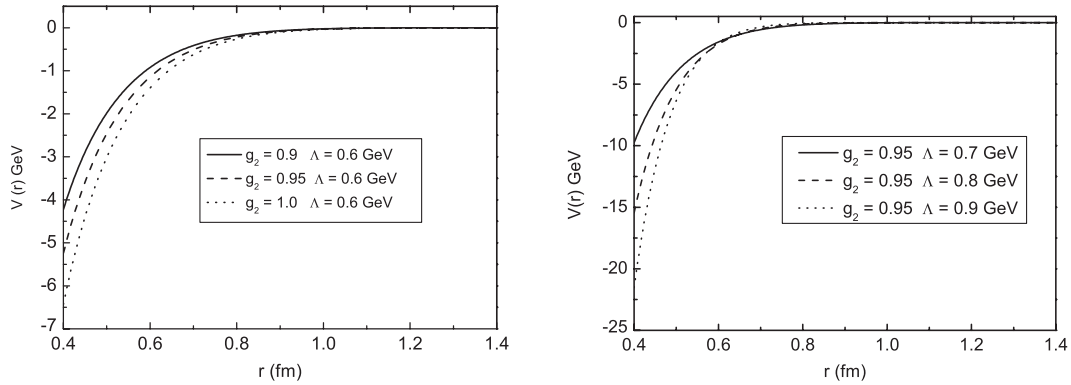

FIG. 3. The $\Lambda_c - \bar{\Lambda}_c$ central potential behavior in the case of a Gaussian form factor versus different parameter choices.

$$V^B_{CG3} = \frac{g_4^4 \Lambda^3 m^{5/2} e^{m^2/\Lambda^2}}{32\sqrt{2}\pi^3 f_\pi^4 \Delta_1^2 r^{3/2}} e^{-(\Lambda^2 r^2/4) - mr}, \tag{54}$$

$$V^B_{CG4} = \frac{g_4^4 \Lambda^3 m^{3/2} e^{m^2/\Lambda^2}}{16\sqrt{2}\pi^3 f_\pi^4 \Delta_1^2 r^{5/2}} e^{-(\Lambda^2 r^2/4) - mr} - \frac{g_4^4 m^{9/2} e^{2m^2/\Lambda^2}}{128\pi^{5/2} f_\pi^4 \Delta_1^2 r^{5/2}} e^{-2mr}. \tag{55}$$

With Gaussian form factors, it is seen from Eq. (A11) in the Appendix that for a given Λ the function $F(\lambda, r)$ is suppressed for large λ values; that is, the dominant contribution to the potential comes from the small λ region. So, in obtaining the analytic expressions of the above potentials and hereafter, we expand the corresponding functions, as defined in the Appendix, in λ and keep only the leading term. In this approach, the crossed diagram contributes to the potential the same as the box diagram at the leading order in λ expansion, and hence is not presented here.

Similarly, we obtain the potentials from triangle and two-pion loop diagrams, i.e.,

$$V^T_{CG5} = \frac{g_4^2 m \Lambda^3}{32\sqrt{2}\pi^{7/2} f_\pi^4 \Delta_1 r^2} e^{-(\Lambda^2 r^2/2)} - \frac{g_4^2 m^{5/2} \Lambda e^{m^2/\Lambda^2}}{16\sqrt{2}\pi^3 f_\pi^4 \Delta_1 r^{5/2}} e^{-(\Lambda^2 r^2/4) - mr} + \frac{g_4^2 m^{7/2} e^{2m^2/\Lambda^2}}{128\pi^{5/2} f_\pi^4 \Delta_1 r^{5/2}} e^{-2mr}, \tag{56}$$

and

$$V^L_{CG6} = -\frac{m^{1/2} \Lambda^3}{32\sqrt{2}\pi^2 f_\pi^4 r^{3/2}} e^{-(1/4)\Lambda^2 r^2 - mr}. \tag{57}$$

To get the central potential for the case of the spin-$\frac{1}{2}$ intermediate state, one needs only to make the following replacement,

$$g_4 \to g_2, \qquad \Delta_1 \to \Delta_1' = M_{\Sigma_c} - M_{\Lambda_c}, \tag{58}$$

in Eq. (50).

Note that in the above asymptotic expressions we keep only those terms up to order $r^{5/2}$, and more singular terms are not taken into account in this work. The dependence of the potential on various parameters is shown in Fig. 3. The results indicate that the potential approaches zero quickly

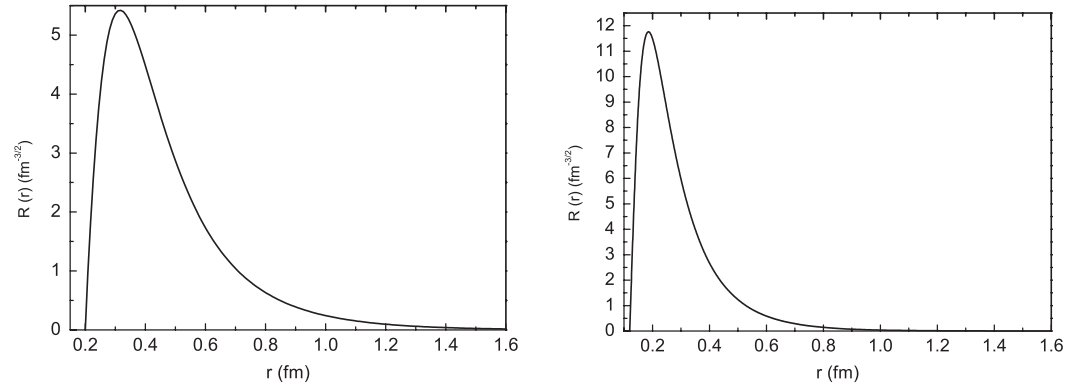

FIG. 4. Radial wave function of the $\Lambda_c - \bar{\Lambda}_c$ ground state. The left figure is for the case of a Gaussian form factor under the conditions $|g_2| = 0.95$ and $\Lambda = 0.8$, and the right one is for the case of a monopole form factor with $|g_2| = 0.9$ and $\Lambda = 0.95$.

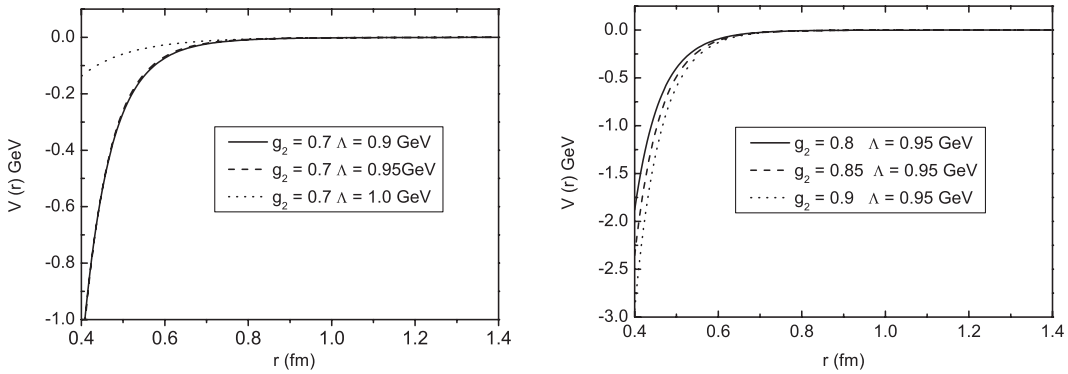

FIG. 5. The $\Lambda_c - \bar{\Lambda}_c$ central potential behavior in the case of a monopole form factor versus different choices of inputs.

in the long range in every case, while in the short range the potential diverges very much with different parameters, as expected. As a result, the binding energy heavily depends on the coupling constants and the cutoff. One can read from the figure that, in the small coupling situation, the potential becomes too narrow and shallow to bind two heavy baryons. Table II presents the binding energies of the $\Lambda_c - \bar{\Lambda}_c$ and $\Sigma_c - \bar{\Sigma}_c$ systems with different inputs. Schematically, the radial wave functions for the ground state of the $\Lambda_c - \bar{\Lambda}_c$ system with Gaussian and monopole form factors are shown in Fig. 4, while the wave functions for the $\Sigma_c - \bar{\Sigma}_c$ system have similar curves.

B. Monopole form factor case

In order to regulate the singularities at the origin in configuration space, people usually employ three types of form factors in the literature, i.e. the Gaussian, the monopole, and the dipole form factors [34]. For comparison, we also calculate the potential with the monopole form factor using the same factorization technique, and the basic Fourier transformation for the monopole form factor is presented in the Appendix for the sake of convenience. Here, in obtaining the analytic expressions for the potentials, we also expand the corresponding functions in parameter λ and keeping only the leading term. Then, from the box-diagram contribution we get

$$V^B_{CM}(r) = -\frac{g_4^4}{8\pi^{5/2} f_\pi^4 \Delta^2 r^{5/2}}\left(\frac{m^{9/2}}{4} e^{-2mr} + \frac{\Lambda^4 m^{1/2}}{4} e^{-2\Lambda r}\right) + \frac{g_4^4 \Lambda^{5/2} m^{5/2}}{8\sqrt{2}\pi^{5/2} f_\pi^4 \sqrt{m+\Lambda}\Delta_1^2 r^{5/2}} e^{-(m+\Lambda)r}. \quad (59)$$

Contributions from triangle and two-pion loop diagrams are

$$V^T_{CM}(r) = \frac{g_4^2 m^{7/2}}{16\pi^{5/2} f_\pi^4 \Delta_1 r^{5/2}} e^{-2mr} + \frac{g_4^2 m \Lambda^{5/2}}{16\pi^{5/2} f_\pi^4 \Delta_1 r^{5/2}} e^{-2\Lambda r} - \frac{g_4^2 m^{5/2} \Lambda^{3/2}}{4\sqrt{2}\pi^{5/2} f_\pi^4 \sqrt{m+\Lambda}\Delta_1 r^{5/2}} e^{-(m+\Lambda)r} \quad (60)$$

and

$$V^L_{CM}(r) = -\frac{(\Lambda^2 - m^2) m^{1/2}}{32\sqrt{2}\pi^{3/2} f_\pi^4 r^{3/2}} e^{-(m+\Lambda)r} + \frac{(\Lambda^2 - m^2)\Lambda^{1/2}}{32\sqrt{2}\pi^{3/2} f_\pi^4 r^{3/2}} e^{-2\Lambda r}, \quad (61)$$

respectively, where the superscripts B, T, and L stand for box, triangle, and 2π loop. Note that since there is no heavy baryon intermediate state in the 2π loop process, as shown in the right graph of Fig. 2, its potential range appears to be different.

We find that the structure of the potential with a monopole form factor is much simpler than the Gaussian case. The dependence of the potential on various parameters is shown in Fig. 5. From the figure one can see that in the small coupling case the potential changes less, which means the potential tends to be insensitive to the small

TABLE II. Binding energies with different inputs using the Gaussian form factor. The upper table is for the $\Lambda_c - \bar{\Lambda}_c$ system, and the lower one is for the $\Sigma_c - \bar{\Sigma}_c$ system.

$\lvert g_2\rvert$	Λ(GeV)	Binding energy	Baryonium mass
<0.9	<0.6	No	⋯
0.9	0.6	−22 MeV	4.550 GeV
0.95	0.6	−77 MeV	4.495 GeV
1.0	0.6	−168 MeV	4.404 GeV
0.95	0.7	−196 MeV	4.376 GeV
0.95	0.8	−227 MeV	4.345 GeV
0.95	0.9	−588 MeV	3.984 GeV

g_1	Λ(GeV)	Binding energy	Baryonium mass
<1.0	<0.8	No	⋯
1.0	0.8	−11 MeV	4.895 GeV
1.05	0.8	−61 MeV	4.845 GeV
1.1	0.8	−145 MeV	4.761 GeV
1.05	0.85	−141 MeV	4.765 GeV
1.05	0.9	−266 MeV	4.640 GeV
1.05	0.95	−438 MeV	4.468 GeV

TABLE III. Binding energies with different inputs using the monopole form factor. The upper table is for the $\Lambda_c - \bar{\Lambda}_c$ system, and the lower one is for the $\Sigma_c - \bar{\Sigma}_c$ system.

$\lvert g_2\rvert$	Λ(GeV)	Binding energy	Baryonium mass
<0.7	<0.9	No	...
0.8	0.95	-117 MeV	4.455 GeV
0.85	0.95	-420 MeV	4.152 GeV
0.9	0.95	-521 MeV	4.051 GeV
0.7	0.9	-5 MeV	4.567 GeV
0.7	0.95	-67 MeV	4.505 GeV
0.7	1.0	-252 MeV	4.320 GeV

g_1	Λ(GeV)	Binding energy	Baryonium mass
<0.9	<0.9	No	
0.95	0.95	-438 MeV	4.468 GeV
1.0	0.95	-830 MeV	4.076 GeV
1.05	0.95	-1003 MeV	3.903 GeV
0.9	0.9	-40 MeV	4.866 GeV
0.9	0.95	-153 MeV	4.753 GeV
0.9	1.0	-345 MeV	4.561 GeV

coupling, and hence the binding energy. Solving the Schrödinger equation we then obtain eigenvalues for different input parameters, given in Table III. From the table, we notice that the binding energy is sensitive to and changes greatly with the variation of g_1, $|g_2|$, and the cutoff Λ, the same as in the case with a Gaussian form factor. Intuitively, the realistic baryonium can only accommodate small ones of those parameters.

TABLE IV. Binding energies with the change of parameters for the Λ_b-$\bar{\Lambda}_b$ system. The upper table is for the Gaussian form factor, and the lower one is for the monopole form factor. Here g_b corresponds to g_2 in the charmed baryonium sector.

$\lvert g_b\rvert$	Λ(GeV)	Binding energy	Baryonium mass
<0.7	<0.7	No	No
0.7	0.75	-4 MeV	11.236 GeV
0.8	0.75	-76 MeV	11.164 GeV
0.9	0.75	-294 MeV	10.946 GeV
0.8	0.8	-164 MeV	11.706 GeV
0.8	0.9	-396 MeV	10.844 GeV
0.8	1.0	-622 MeV	10.618 GeV

$\lvert g_b\rvert$	Λ(MeV)	Binding energy	Baryonium mass
<1.0	<0.8	No	No
1.0	0.8	-11 MeV	11.229 GeV
1.05	0.8	$-56Mev$	11.184 GeV
1.1	0.8	-143 MeV	11.097 GeV
1.05	0.8	$-103Mev$	11.137 GeV
1.05	0.9	-164 MeV	11.076 GeV
1.05	1.0	-321 MeV	10.919 GeV

C. Ground state of $\Lambda_b - \bar{\Lambda}_b$ baryonium

We also estimate the ground state of the $\Lambda_b - \bar{\Lambda}_b$ baryonium system with Gaussian and monopole form factors. The results are shown in Table IV, where g_b corresponds to g_2 in the charmed baryonium sector. Note that the dominant decay mode of Σ_b is to $\Lambda_b\pi$, by which we may constrain the $\Sigma_b\Lambda_b\pi$ coupling from the experiment result, and this may shed light on a further investigation of the possible nature of baryonium.

IV. SUMMARY AND CONCLUSIONS

In the framework of heavy baryon chiral perturbation theory we have studied the heavy baryon-baryon interaction and obtained the interaction potential, the central potential, in the case of two-pion exchange. The Gaussian and monopole form factors are employed to regularize the loop integrals in the calculation. As a leading order analysis, the tensor potential and higher order contributions in the $\frac{1}{M_H}$ expansion are neglected. As expected, we found that the potential is sensitive to the baryon-pion couplings and the energy cutoff Λ used in the form factor.

We apply the obtained potential to the Schrödinger equation in attempting to see whether the attraction of the two-pion-exchange potential is large enough to constrain two heavy baryons into baryonium. We find that it is large enough for a reasonable choice of cutoff Λ and baryon-pion couplings, which is quite different from the conclusion of a recent work in the study of the $D\bar{D}$ potential through two-pion exchange [35]. Since usually the cutoff Λ is taken to be less than the nucleon mass, i.e. about 1 GeV in the literature, in our calculation we adopt a similar value to that employed in the nucleon-nucleon case. In Ref. [35] the authors took a fixed coupling $g = 0.59$ and obtained the binding with a large cutoff, while in our calculation for the baryonium system with a Gaussian form factor, there will be no binding when $g_1 < 1.0$ and $\Lambda < 0.8$. The increase of the coupling constant will lead to an even smaller Λ for a given binding energy.

Based on our calculations it is interesting to note that if there exists binding in the $\Sigma_c - \bar{\Sigma}_c$ system, with both Gaussian and monopole factors, the coupling g_1 will be much bigger than what was conjectured in Ref. [25]. However, for the $\Lambda_c - \bar{\Lambda}_c$ system, to form a bound state the baryon-Goldstone coupling g_2 could be similar in magnitude to what was estimated in the literature.

Notice that the potential depends not only on the coupling constants and the cutoff Λ, but also on the types of form factors employed. Our calculation indicates that the Gaussian form factor and the monopole form factor are similar in regulating the singularities at the origin, and they lead to similar results, with only subtle differences, for both the Λ_c and Λ_b systems. Numerical results show that the heavy baryon-baryon potentials are more sensitive to the coupling constants in the case of the monopole form

factor, but are more sensitive to the cutoff Λ in the case of the Gaussian form factor. From our calculation it is tempting to conjecture that the recently observed states $Y(4260)$ and $Y(4360)$, but not $Y(4660)$ [6], in the charm sector could be a $\Lambda_c - \bar{\Lambda}_c$ bound state with a reasonable amount of binding energy, which deserves a further investigation. Our result also shows that the newly observed exotic state in the bottom sector, the $Y_b(10890)$ [36], could be treated as the $\Lambda_b - \bar{\Lambda}_b$ bound state, with an extremely large binding energy.

It is worth emphasizing at this point that, although our result favors the existence of heavy baryonium, it is still hard to make a definite conclusion yet, especially with only the leading order two-pion-exchange potential. The potential sensitivity on the coupling constants and energy cutoff also looks unusual and needs further investigation. To be closer to the truth, one needs to go beyond the leading order of accuracy in $\frac{1}{M_H}$ expansion; one should also investigate the potential while two baryonlike triquark clusters carry colors as proposed in the heavy baryonium model [11,15]; last, but not least, the unknown and difficult to evaluate annihilation channel effect on the heavy baryonium potential should also be clarified, especially for a heavy baryon-antibaryon interaction, which nevertheless could be phenomenologically parametrized so as to reproduce known widths of some observed states.

ACKNOWLEDGMENTS

This work was supported in part by the National Natural Science Foundation of China (NSFC) and by the CAS Key Projects KJCX2-yw-N29 and H92A0200S2.

APPENDIX

In this appendix, we present more detailed formulas and definitions for the sake of the reader's convenience.

The γ matrices take the following convention:

$$\gamma^0 = \begin{pmatrix} 1 & 0 \\ 0 & -1 \end{pmatrix}, \quad \gamma^i = \begin{pmatrix} 0 & \sigma^i \\ -\sigma^i & 0 \end{pmatrix}, \quad \gamma_5 = \begin{pmatrix} 0 & 1 \\ 1 & 0 \end{pmatrix}. \tag{A1}$$

And the Dirac spinors for Σ_c read as

$$u(p) = \sqrt{\frac{E + M_\Sigma}{2M_\Sigma}} \begin{pmatrix} \chi_a \\ \frac{\boldsymbol{\sigma}\cdot\mathbf{p}}{E+M_\Sigma}\chi_a \end{pmatrix}, \tag{A2}$$

where χ_a is a two-component Pauli spinor, and

$$v(p) = \sqrt{\frac{E + M_\Sigma}{2M_\Sigma}} \begin{pmatrix} \frac{\boldsymbol{\sigma}\cdot\mathbf{p}}{E+M_\Sigma}\eta_a \\ \eta_a \end{pmatrix}, \tag{A3}$$

where $\eta_a = -i\sigma^2\chi_a^*$ and $a = 1, 2$. The spin-$\frac{3}{2}$ field for Σ^{+*} is described by the Rarita-Schwinger spinor $u^\mu(p, \sigma)$, which can be constructed by the spin-1 vector and spin-$\frac{1}{2}$ field [37], that is,

$$u^\mu = \sqrt{\frac{E + M_{\Sigma^{+*}}}{2M_{\Sigma^{+*}}}} L^{(1)}(p)^\mu_\nu \begin{pmatrix} 1 \\ \frac{\boldsymbol{\sigma}\cdot\mathbf{p}}{E+M_{\Sigma^{+*}}} \end{pmatrix} S^{\dagger\nu}\psi(\sigma), \tag{A4}$$

where $\psi(\sigma)$ is a four-component Pauli spinor of a spin-$\frac{3}{2}$ particle, and $L^{(1)}(p)^\mu_\nu$ is the boost operator for a spin-1 particle,

$$L^{(1)}(p)^\mu_\nu = \begin{pmatrix} \frac{E}{M_{\Sigma^{+*}}} & \frac{p_j}{M_{\Sigma^{+*}}} \\ \frac{p_i}{M_{\Sigma^{+*}}} & \delta^i_j - \frac{p^i p_j}{M_{\Sigma^{+*}}(E+M_{\Sigma^{+*}})} \end{pmatrix}, \tag{A5}$$

where i, j are indices of the space components of momentum p. The positive- and negative-energy projection operators for the spin-$\frac{1}{2}$ baryon are

$$[\Lambda^+(p)]_{\alpha\beta} = \sum_{\pm s} u_\alpha(p, s)\bar{u}_\beta(p, s) = \left(\frac{\not{p} + M_{\Sigma_c}}{2M_{\Sigma_c}}\right)_{\alpha\beta} \tag{A6}$$

and

$$[\Lambda^-(p)]_{\alpha\beta} = -\sum_{\pm s} v_\alpha(p, s)\bar{v}_\beta(p, s) = \left(\frac{-\not{p} + M_{\Sigma_c}}{2M_{\Sigma_c}}\right)_{\alpha\beta}, \tag{A7}$$

respectively.

The positive- and negative-energy projection operators for the spin-$\frac{3}{2}$ baryon are

$$\begin{aligned}[\Lambda^+_{\mu\nu}(p)]_{\alpha\beta} &= \sum_{\pm s} u_{\mu,\alpha}(p, s)\bar{u}_{\nu,\beta}(p, s) \\ &= \left[\frac{\not{p} + M_{\Sigma_c^*}}{2M_{\Sigma_c^*}}\right]_{\alpha\beta}\left(g_{\mu\nu} - \frac{\gamma_\mu\gamma_\nu}{3} - \frac{2p_\mu p_\nu}{3M^2_{\Sigma_c^*}} + \frac{p_\mu\gamma_\nu - p_\nu\gamma_\mu}{3M_{\Sigma_c^*}}\right)\end{aligned} \tag{A8}$$

and

$$\begin{aligned}[\Lambda^-_{\mu\nu}(p)]_{\alpha\beta} &= -\sum_{\pm s} v_{\mu,\alpha}(p, s)\bar{v}_{\nu,\beta}(p, s) \\ &= \left[\frac{-\not{p} + M_{\Sigma_c^*}}{2M_{\Sigma_c^*}}\right]_{\alpha\beta}\left(g_{\mu\nu} - \frac{\gamma_\mu\gamma_\nu}{3} - \frac{2p_\mu p_\nu}{3M^2_{\Sigma_c^*}} + \frac{p_\mu\gamma_\nu - p_\nu\gamma_\mu}{3M_{\Sigma_c^*}}\right),\end{aligned} \tag{A9}$$

respectively. Here, μ and ν are Lorentz indices; α and β are Dirac spinor indices.

The basic Fourier transformation with the Gaussian form factor reads

$$\begin{aligned}I_2(m, r) &= \int_{-\infty}^{\infty} \frac{d^3\mathbf{k}}{(2\pi)^3} \frac{e^{i\mathbf{k}\mathbf{r}} e^{-\mathbf{k}^2/\Lambda^2}}{\mathbf{k}^2 + m^2} \\ &= \frac{1}{8\pi r} e^{m^2/\Lambda^2}\left[e^{-mr} erfc\left(-\frac{\Lambda r}{2} + \frac{m}{\Lambda}\right) - e^{mr} erfc\left(\frac{\Lambda r}{2} + \frac{m}{\Lambda}\right)\right],\end{aligned} \tag{A10}$$

and hence

$$F(\lambda, r) = \int \frac{d^3\mathbf{k}}{(2\pi)^3} \frac{e^{i\mathbf{k}\mathbf{r}} e^{-\mathbf{k}^2/\Lambda^2}}{\mathbf{k}^2 + m^2 + \lambda^2} = I_2(\sqrt{m^2+\lambda^2}, r) e^{-\lambda^2/\Lambda^2}. \tag{A11}$$

The term $erfc(x)$ is a complementary error function, which is defined as

$$erfc(x) = \frac{2}{\sqrt{\pi}} \int_x^\infty e^{-t^2} dt. \tag{A12}$$

The factorization in the double Fourier transformation is

$$\begin{aligned} H_{11} &= \iint \frac{d^3\mathbf{k}_1 d^3\mathbf{k}_2}{(2\pi)^6} \frac{e^{i\mathbf{k}_1\mathbf{r}_1} e^{i\mathbf{k}_2\mathbf{r}_2} f(\mathbf{k}_1^2) f(\mathbf{k}_2^2)}{\omega_1\omega_2(\omega_1+a)(\omega_2+a)(\omega_1+\omega_2)} \\ &= \iint \frac{d^3\mathbf{k}_1 d^3\mathbf{k}_2}{(2\pi)^6} \frac{1}{a^2}\left[\frac{2}{\pi}\int_0^\infty \frac{e^{i\mathbf{k}_1\mathbf{r}_1} e^{i\mathbf{k}_2\mathbf{r}_2} f(\mathbf{k}_1^2) f(\mathbf{k}_2^2) d\lambda}{(\omega_1^2+\lambda^2)(\omega_2^2+\lambda^2)} - \frac{2}{\pi}\int_0^\infty \frac{e^{i\mathbf{k}_1\mathbf{r}_1} e^{i\mathbf{k}_2\mathbf{r}_2} f(\mathbf{k}_1^2) f(\mathbf{k}_2^2) \lambda^2 d\lambda}{(a^2+\lambda^2)(\omega_1^2+\lambda^2)(\omega_2^2+\lambda^2)}\right] - \frac{1}{a} G_{11}(\lambda, r_1) G_{11}(\lambda, r_2) \\ &= \frac{2}{\pi}\int_0^\infty \frac{d\lambda}{a^2+\lambda^2} F(\lambda, r_1) F(\lambda, r_2) - \frac{1}{a} G_{11}(\lambda, r_1) G_{11}(\lambda, r_2). \end{aligned} \tag{A13}$$

Here,

$$G_{11} = \int \frac{d^3\mathbf{k}_1}{(2\pi)^3} \frac{e^{i\mathbf{k}_1\mathbf{r}} e^{-\mathbf{k}_1^2/\Lambda^2}}{\omega_1(\omega_1+a)} = \int \frac{d^3\mathbf{k}_1}{(2\pi)^3} \frac{2a}{\pi} \int_0^\infty \frac{e^{i\mathbf{k}_1\mathbf{r}} e^{-\mathbf{k}_1^2/\Lambda^2} d\lambda}{(a^2+\lambda^2)(\omega_1^2+\lambda^2)} = \frac{2a}{\pi}\int_0^\infty \frac{d\lambda}{(a^2+\lambda^2)} F(\lambda, r), \tag{A14}$$

and for simplicity we define $\omega_1 = \sqrt{\mathbf{k}_1^2 + m^2}$ and $\omega_2 = \sqrt{\mathbf{k}_2^2 + m^2}$.

In the case of the monopole form factor, i.e. $f(\mathbf{k}^2) = \frac{\Lambda^2 - m^2}{\Lambda^2 + \mathbf{k}^2}$, the function that corresponds to $F(\lambda, r)$ reads

$$R(\lambda, r) = \int \frac{d^3\mathbf{k}}{(2\pi)^3} \frac{e^{i\mathbf{k}\mathbf{r}}}{\mathbf{k}^2 + m^2 + \lambda^2} \frac{\Lambda^2 - m^2}{\Lambda^2 + \mathbf{k}^2 + \lambda^2} = \frac{1}{4\pi r}(e^{-r\sqrt{m^2+\lambda^2}} - e^{-r\sqrt{\Lambda^2+\lambda^2}}). \tag{A15}$$

The operator $O_1(\mathbf{k}_1, \mathbf{k}_2)$ contains two parts. The first part of $O_1(\mathbf{k}_1, \mathbf{k}_2)$, while acting on functions in configuration space, is

$$\begin{aligned} O_1(\mathbf{k}_1, \mathbf{k}_2) F(\lambda, r_1) F(\lambda, r_2) &= (\mathbf{k}_1 \cdot \mathbf{k}_2)^2 F(\lambda, r_1) F(\lambda, r_2) = (\nabla_{1i}\nabla_{1j}) F(\lambda, r_1)(\nabla_{2i}\nabla_{2j}) F(\lambda, r_2) \\ &= \frac{2}{r^2} F'(\lambda, r) F'(\lambda, r) + F''(\lambda, r) F''(\lambda, r), \end{aligned} \tag{A16}$$

where

$$\nabla_i \nabla_j = \left(\delta_{ij} - \frac{x_i x_j}{r^2}\right)\left(\frac{1}{r}\frac{d}{dr}\right) + \frac{x_i x_j}{r^2}\left(\frac{d^2}{dr^2}\right), \tag{A17}$$

and the limit $r_2 \to r_1 = r$ is taken. The second part of $O_2(\mathbf{k}_1, \mathbf{k}_2)$, while acting on functions in configuration space, is

$$\begin{aligned} O_2(\mathbf{k}_1, \mathbf{k}_2) F(\lambda, r_1) F(\lambda, r_2) &= (\boldsymbol{\sigma}_1 \cdot \mathbf{k}_1 \times \mathbf{k}_2)(\boldsymbol{\sigma}_2 \cdot \mathbf{k}_1 \times \mathbf{k}_2) F(\lambda, r_1) F(\lambda, r_2) \\ &= \sigma_{1i}\sigma_{2j}\varepsilon_{ikl}\varepsilon_{jmn}(\nabla_{1k}\nabla_{1m}) F(\lambda, r_1)(\nabla_{2l}\nabla_{2n}) F(\lambda, r_2) \\ &= \sigma_{1i}\sigma_{2j}(\delta_{ij}\delta_{km}\delta_{ln} + \delta_{im}\delta_{kn}\delta_{lj} + \delta_{in}\delta_{lm}\delta_{kj} - \delta_{lj}\delta_{km}\delta_{in} - \delta_{lm}\delta_{kn}\delta_{ij} - \delta_{ln}\delta_{im}\delta_{kj}) \\ &\quad \times (\nabla_{1k}\nabla_{1m}) F(\lambda, r_1)(\nabla_{2l}\nabla_{2n}) F(\lambda, r_2) \\ &= \frac{2}{3}\left[\frac{1}{r^2} F'(\lambda, r) F'(\lambda, r) + \frac{2}{r} F'(\lambda, r) F''(\lambda, r)\right](\boldsymbol{\sigma}_1 \cdot \boldsymbol{\sigma}_2) + \frac{2}{3}\left(\frac{F'(\lambda, r)}{r} - F''(\lambda, r)\right)\frac{1}{r} F'(\lambda, r) S_{12}, \end{aligned} \tag{A18}$$

where $\boldsymbol{\sigma}_1 \cdot \boldsymbol{\sigma}_2$ gives the spin-spin potential and $S_{12} = \frac{3(\boldsymbol{\sigma}_1 \cdot \mathbf{r})(\boldsymbol{\sigma}_2 \cdot \mathbf{r})}{r^2} - \boldsymbol{\sigma}_1 \cdot \boldsymbol{\sigma}_2$ gives the tensor potential.

[1] W. Lucha, F. F. Schöberl, and D. Gromes, Phys. Rep. **200**, 127 (1991).
[2] C. Quigg and J. L. Rosner, Phys. Rep. **56**, 167 (1979).
[3] V. A. Novikov, L. B. Okun, M. A. Shifman, A. I. Vainshtein, M. B. Voloshin, and V. I. Zakharov, Phys. Rep. **41**, 1 (1978).
[4] S. K. Choi *et al.* (Belle Collaboration), Phys. Rev. Lett. **91**, 262001 (2003).
[5] B. Aubert *et al.* (*BABAR* Collaboration), Phys. Rev. D **77**, 111101 (2008).
[6] B. Aubert *et al.* (*BABAR* Collaboration), Phys. Rev. Lett. **98**, 212001 (2007); X. L. Wang *et al.* (Belle Collaboration), Phys. Rev. Lett. **99**, 142002 (2007); S. K. Choi *et al.* (Belle Collaboration), Phys. Rev. Lett. **100**, 142001 (2008); R. Mizuk *et al.* (Belle Collaboration), Phys. Rev. D **80**, 031104 (2009).
[7] S. L. Zhu, Phys. Lett. B **625**, 212 (2005); E. Kou and O. Pene, Phys. Lett. B **631**, 164 (2005); F. E. Close and P. R. Page, Phys. Lett. B **628**, 215 (2005); X. Q. Luo and Y. Liu, Phys. Rev. D **74**, 034502 (2006); S. L. Zhu, Nucl. Phys. **A805**, 221c (2008); S. L. Zhu, Int. J. Mod. Phys. E **17**, 283 (2008).
[8] X. Liu, X. Q. Zeng, and X. Q. Li, Phys. Rev. D **72**, 054023 (2005).
[9] F. J. Llanes-Estrada, Phys. Rev. D **72**, 031503 (2005).
[10] C.-Z. Yuan, P. Wang, and X. H. Mo, Phys. Lett. B **634**, 399 (2006).
[11] C.-F. Qiao, Phys. Lett. B **639**, 263 (2006).
[12] G.-J. Ding, Phys. Rev. D **79**, 014001 (2009).
[13] L. Maiani, V. Riquer, F. Piccinini, and A. D. Polosa, Phys. Rev. D **72**, 031502(R) (2005).
[14] G.-J. Ding, J.-J. Zhu, and M.-L. Yan, Phys. Rev. D **77**, 014033 (2008).
[15] C.-F. Qiao, J. Phys. G **35**, 075008 (2008).
[16] B.-Q. Li and and K.-T. Chao, Phys. Rev. D **79**, 094004 (2009).
[17] D. V. Bugg, J. Phys. G **36**, 075002 (2009).
[18] F.-K. Guo, C. Hanhart, and U.-G. Meißner, Phys. Lett. B **665**, 26 (2008).
[19] Z.-G. Wang and X.-H. Zhang, Commun. Theor. Phys. **54**, 323 (2010).
[20] A. M. Badalian, B. L. G. Bakker, and I. V. Danilkin, Phys. At. Nucl. **72**, 638 (2009).
[21] R. M. Albuquerque and M. Nielsen, Nucl. Phys. **A815**, 53 (2009).
[22] D. Ebert, R. N. Faustov, and V. O. Galkin, Eur. Phys. J. C **58**, 399 (2008).
[23] N. Brambilla *et al.*, Eur. Phys. J. C **71**, 1 (2011).
[24] N. Drenska *et al.*, Riv. Nuovo Cimento **033**, 633 (2010).
[25] Tung-Mow Yan, Y. C. Lin, and Hoi-Lai Yu, Phys. Rev. D **46**, 1148 (1992); Hai-Yang Cheng *et al.*, Phys. Rev. D **47**, 1030 (1993).
[26] A. Manohar and H. Georgi, Nucl. Phys. **B234**, 189 (1984).
[27] M. B. Wise, Phys. Rev. D **45**, R2188 (1992).
[28] Th. A. Rijken and V. G. J. Stoks, Phys. Rev. C **46**, 73 (1992); **46**, 102 (1992).
[29] Th. A. Rijken, Ann. Phys. (N.Y.) **208**, 253 (1991).
[30] Th. A. Rijken and V. G. Stoks, Phys. Rev. C **54**, 2869 (1996).
[31] http://users.ugent.be/~vledoux/.
[32] K. Nakamura *et al.* (Particle Date Group), J. Phys. G **37**, 075021 (2010).
[33] D. Arndt, S. R. Beane, and M. J. Savage, Nucl. Phys. **A726**, 339 (2003); S. R. Beane and M. J. Savage, Phys. Lett. B **556**, 142 (2003).
[34] V. G. J. Stoks, R. A. M. Klomp, C. P. F. Terheggen, and J. J. de Swart, Phys. Rev. C **49**, 2950 (1994).
[35] Q. Xu, G. Liu, and H.-Y. Jin, arXiv:hep-ph/1012.5949.
[36] K. F. Chen *et al.* (Belle Collaboration), Phys. Rev. Lett. **100**, 112001 (2008).
[37] Th. A. Rijken and V. G. Stoks, Phys. Rev. C **46**, 102 (1992).